

Accepted Manuscript

A novel viscoelastic damping treatment for honeycomb sandwich structures

P. Aumjaud, C.W. Smith, K.E. Evans

PII: S0263-8223(14)00438-3

DOI: <http://dx.doi.org/10.1016/j.compstruct.2014.09.005>

Reference: COST 5881

To appear in: *Composite Structures*



Please cite this article as: Aumjaud, P., Smith, C.W., Evans, K.E., A novel viscoelastic damping treatment for honeycomb sandwich structures, *Composite Structures* (2014), doi: <http://dx.doi.org/10.1016/j.compstruct.2014.09.005>

This is a PDF file of an unedited manuscript that has been accepted for publication. As a service to our customers we are providing this early version of the manuscript. The manuscript will undergo copyediting, typesetting, and review of the resulting proof before it is published in its final form. Please note that during the production process errors may be discovered which could affect the content, and all legal disclaimers that apply to the journal pertain.

A novel viscoelastic damping treatment for honeycomb sandwich structures.

P. Aumjaud, C.W. Smith*, K.E. Evans.

College of Engineering, Mathematics and Physical Sciences, University of Exeter, Exeter EX4 4QF, UK.

Abstract:

Constrained layer dampers (CLD) are in widespread use for passive vibration damping, in applications including aerospace structures which are often lightweight. The location and dimensions of CLD devices on structures has been the target of several optimisation studies using a variety of techniques such as genetic algorithms, cellular automata, and gradient techniques. The recently developed Double Shear Lap-Joint (DSLJ) damper is an alternative method for vibration damping, and can be placed internally within structures. The performance of the DSLJ damper is compared in a parametric study with that of CLD dampers on beam and plate structures under both cantilever and simply supported boundary conditions, using finite element analysis. The objective was to determine which damper and in which configuration produced the highest modal loss factor and amplitude reduction for least added mass, as would be important for lightweight applications. The DSLJ tend to be more mass efficient in terms of loss factor and amplitude reduction for cantilevered beam and plate structure, and are competitive with CLD dampers in simply supported beam and plate structures. The DSLJ works well because it has the potential to magnify global flexural deformation into shear deformation in the viscoelastic more effectively than traditional CLD dampers.

Keywords: honeycomb, damping, viscoelastic, double shear lap-joint damper

* Corresponding author. Tel.: +44 1392263652.

E-mail address: c.w.smith@ex.ac.uk (C.W. Smith).

1. Introduction

Sandwich structures are widely used in the aerospace, aeronautical and automotive industries for their high strength and stiffness-to-mass ratio [1]. These environments are often vibration rich, which can make fatigue problematic, reduce fuel efficiency, and adversely affect passenger comfort. A common mitigation technique is to damp vibrations via methods such as Constrained Layer Dampers (CLD), which consist of a thin layer of viscoelastic material adhered to the vibrating structure and a constraining stiff layer on its surface. This arrangement constrains the viscoelastic layer to deform in shear and at relatively higher strain thereby efficiently dissipating vibration energy as heat [2]. Recently, the damping properties of load bearing structures have been enhanced by inserting viscoelastic material in constructs that constrain it in shear and therefore maximise the loss mechanism. Star-shaped inclusions filled with viscoelastic material [3], elastomer inserts at the acute vertices of a auxetic honeycomb cell [4] and viscoelastic ligament between opposite vertex of a honeycomb cell [5], [6] have all proven their efficacy for vibration damping. A new type of viscoelastic damping device termed the double shear lap joint (DSLJ) has been developed which may offer an alternative to the CLD [5], [7]. All such devices add mass to their host structures, and in very lightweight structures this might be expected to reduce natural frequencies, which may be adverse where structures have been tuned to avoid resonance in normal operation.

The design of a CLD was first proposed by Kerwin [8] in 1959 who examined the damping of flexural vibrations of a stiff simply supported beam structure with a continuous viscoelastic layer.–The contiguous layer CLDs are effective in damping vibrations but may add significant extra mass to lightweight structures. To tackle this problem discrete CLD patches were developed where the host structure was only partially covered with dampers, proving to be more mass efficient designs than complete coverage. Nokes and Nelson [9] were among the first to investigate partial coverage with CLDs and showed both theoretically and experimentally that more efficient damping was possible for partially covered beams.

A number of studies optimising CLD location and dimensions have sought to maximise damping while minimising added mass. There are several parameters one could consider when attempting to quantify ‘damping’ in such optimisation studies, such as vibration amplitude, vibrational energy, and shift in natural frequency, depending on the nature of the application in question. Lifshitz and Leibowitz [10] were the first to apply optimisation techniques to damping of structures, and they used an equality constrained minimisation technique to identify optimal thicknesses, and therefore minimum additional mass, of CLDs on a cantilever beam under a range of constraints on mass and flexural stiffness of the host structure. Both a global criterion method and a genetic algorithm were used by Hajela and Lin [11] to optimise CLDs on a cantilever beam, with the objective being highest modal loss factor and minimal increase in mass. Marcelin et al. [12] used the Method of Moving Asymptotes to find the highest modal loss factor and best location of CLD of a cantilever beam. Zheng and co-workers proposed optimal layouts of CLDs on simply supported beams minimised for amplitude of vibration [13] and for vibrational energy [14], while minimising the damping material volume. Chen and Huang [15] considered the shift of the resonance frequency due to the addition of the damper as a constraint for their optimisation. They proposed an optimised solution for the position of CLD on simply supported plates thanks to a topographical optimisation method. The cellular automaton method is particularly well suited to this problem, and has been implemented by Chia et al. [16], [17] to identify optimal weight-efficient CLD configurations for plates with free

boundary conditions using the loss factor as objective function. Kim also used a topology optimisation in order to find the best configuration of CLD on a fully clamped and cantilevered plate [18] that give the highest modal loss factor for a minimal increase in mass. A Genetic Algorithm was used by Hou et al. in order to minimise the vibrational energy of a simply supported beam [19] and plate [20] damped with CLD. The location of the CLDs was determined with a restriction on the mass added. Ling et al. [21] used the Method of the Moving Asymptotes to determine the optimal layout of CLD on a cantilever and simply supported plate in order to maximise the damping ratio while minimising the added mass. Finally, Zheng et al. [22] had a similar approach considering the maximisation of the modal loss factor. Several studies on damping have used the Modal Strain Energy method developed by Johnson and Kienholtz [23] to calculate the modal loss factor of a structure under harmonic excitation. An alternative and potentially more accurate method to calculate the modal loss factor is the Half-Power Bandwidth approach [24].

The DSLJ damper developed by Boucher *et al.* [5], [7] consists of a double shear lap-joint construct located internally in a structure so that flexure of the host structure results in deformation of the arms of the lap joint and thus shear in the viscoelastic. Boucher considered it within a hexagonal cell core sandwich panel. Both the deformed and undeformed CLD and DSLJ dampers are sketched in Fig. 1. The objective of the present work is to identify the most mass efficient configurations of the CLD and DSLJ devices via simulation using the finite element method. Specifically this is done within a simplified honeycomb sandwich host structure, under typical boundary conditions, utilising a 'lossy' material - in this case a viscoelastic elastomer. The efficiency of the CLD and the DSLJ damper is compared in beam and plate structures with simply supported and cantilever boundary conditions.

2. Methodology

The systems considered here were honeycomb-cored sandwich panels as illustrated in Fig. 2, being typical examples of lightweight high performance structures, and specifically beam and the plate structures, in this case composed of 18 x 2 and 20 x 10 cells respectively. For the cantilevered cases all nodes along the short edge were encastred (i.e. $u_1=u_2=u_3=r_1=r_2=r_3=0$), and for the simply supported case nodes on the bottom surface along lines across the width (i.e. where the knife edge supports would contact) were constrained with no translational freedom but retaining rotational freedom, i.e. $u_1=u_2=u_3=0$, following Srinivas [25]. The honeycomb cells were regular hexagons, with depth and side lengths of 10 mm which is fairly typical of such honeycombs in use in the aerospace sector. The thickness of the honeycomb cell walls and the outer skins was 0.2 mm. The beam's length and width were 270 mm and 34.6 mm respectively (shown in Fig. 2), and the plate's length and width were 300 and 173 mm respectively. This gives length to depth aspect ratios of 27:1 for the beams 30:1 for the plates. The panel skins were considered to be thin (2% of the panel's depth), and made of the same material as the honeycomb cells (aluminium in this case). The DSLJ insert has a depth of 8 mm, and is positioned so as to stand 1 mm away from the upper and lower skins, as illustrated in Fig. 1, to prevent contact with the skins under flexure. The total thickness of the DSLJ damper is 3.2 mm, of which the central aluminium web is 0.2 mm. The viscoelastic material density was approximately a third of the aluminium density, its modulus 70 000 times lower than aluminium, and had a material loss factor 200 times higher than aluminium. These values sits within

the normal range of viscoelastic polymer material properties [16]. Material-dependant damping (ANSYS command MP, DMPR) was adopted to describe the damping ratio of each material. The material properties are given in table 1. The Modal Strain Energy method [23] was used to estimate the modal loss factor of the structure. Although it is known this method may give an inaccurate estimation of the value of the modal loss factor, especially for material's with loss factors, it can efficiently provide a relative comparison of damping between different models. More accurate estimation techniques such as the Modified Modal Strain Energy method [26] would add complexity without necessarily aiding comparison between the different devices presented in this study. A similar approach was adopted by Chia et al. [16]. Douglas and Yang [27] formulated the frequency-dependant complex shear modulus of the viscoelastic core of a constrained layer damper as $G_v^*(\omega) = 0.142 \left(\frac{\omega}{2\pi}\right)^{0.494} (1 + 1.46i)$ MPa. For the range of frequency considered in this study (100 to 560 Hz), the storage modulus would vary between 1.4 MPa and 3.2 MPa. Hence the frequency dependence of the storage and loss moduli can be neglected in this study.

The structure was modelled in three dimensions using the commercial Finite Element software ANSYS 14.0 [28] typically with in the order of 40 000 elements depending on specific geometry and convergence tests. The honeycomb walls in the core and the sandwich skins were modelled as discrete parts, and meshed with a four-noded shell element (Shell181 in ANSYS), which allows flexure in both the honeycomb cell walls and the sandwich skins. The viscoelastic material and the constraining upper layer in the CLDs were meshed with a solid hexahedra or 'brick' element (Solid185 in ANSYS) which has 8 nodes with 3 degrees of freedom. The contact interaction between solid and shell elements required to overlap the contact surfaces in order to ensure the nodes to be coincident at the interface. The degrees of freedom of these nodes were then coupled using the ANSYS command CPINTF in order to enforce compatibility at the interface, similar to the approach adopted by Chia *et al.* [16]. The enhanced strain formulation was used to overcome shear locking in this bending-dominated problem.

Preliminary results indicated that for both beams and plates in both the cantilevered and simply supported modes, the first mode accounts for the largest fraction of the effective mass when the 10 first modes are considered. Hence only the first mode was considered further. Modal analysis was used to explore the effect of the addition of mass and extra stiffness on the mode shape and frequency of the beams and plates. The structure was then excited harmonically at its natural frequency, at the tip for a cantilever structure and at the middle for a simply supported structure in order to excite the first bending mode. The structure's harmonic response was obtained by modal superposition method [28]. Thirty frequency increments were considered in each load step around the natural frequency peak and the cyclic load was also stepped (i.e. the same value is used for all substeps) and chosen with an amplitude of 0.0001 N. The first 5 modes were included in the mode superposition harmonic analysis.

2.1. Parametric optimisation of DSLJ inserts

A method for identification of the optimal position of a damper on a vibrating structure is to locate the area of maximal strain energy via the Modal Strain Energy method, as for example by Marcellin et al. [12]. Therefore, DSLJ dampers might be placed rationally at locations of high modal curvature

[24] i.e. near the clamped edge for a cantilever structure and at the middle for a simply supported structure. A parametric optimisation was used based on this approach to identify the most efficient number of DSLJ inserts on the cantilever and simply supported beam and plate structures. Rows of honeycomb cells were filled with DSLJ inserts sequentially, starting at the clamped end for the cantilever geometries, and from the middle for the simply supported geometries. The evolution of the modal loss factor with the increase in mass was recorded and an optimal number of DSLJ inserts was identified for each configuration based on the loss efficiency E_η (defined in eq. 2 below). A further parametric study was used to determine the optimal thickness of the viscoelastic element in the DSLJ dampers, which was varied between 0.25 to 2.33mm.

2.2. CLD and DSLJ dampers comparison

The present analysis is essentially a comparison of two damping structures, CLDs and DSLJ, identified from the literature, using the Finite Element method to calculate the amplitude, frequency and modal loss factor both before and after the addition of the dampers onto the honeycomb-cored sandwich structures. Hybrid dampers were also included, i.e. those utilising active elements such as piezos, which form part of a sensing and actuation device. However these were only considered in the passive mode, i.e. their active elements were not switched on. The literature hybrid CLD damper configurations had been through an optimisation process, albeit in the active mode.

The CLD optimisation studies from the literature [11]–[15], [18]–[22], [29] presented their optimal CLD configurations in slightly different formats. They were adapted to conform to either a beam or plate structure and in a consistent format for ease of comparison. The dimensions and locations of CLDs were taken from the original studies and implemented *pro rata* on the beam and plate used herein, as illustrated in tables 2a and 2b respectively. For example, Hou *et al.* [19] identified a CLD which stretched from 0.4 to 0.5159 of the total length of their simply supported beam, and this was reconfigured to be the same proportion of the beam used in this study. Some of the literature studies did not optimise parameters such as the thickness of the viscoelastic layer (for example Zheng), but will be explored and optimised in this study. A single core configuration was used across all beam and plate cases, as shown in Fig 2. For information the objective and penalty functions and the design variables used in each literature study are also given in table 2. The vibration amplitude and frequency of the first mode was first computed and the change in amplitude and frequency was compared across the literature CLD and DLSJ configurations. Mass-efficient configurations were identified for each structures and set of boundary conditions. The amplitude reduction efficiency E_a was defined as follows:

$$E_a = \frac{A}{m_a} \quad (1)$$

Where A is the amplitude reduction relative to the undamped structure and m_a is the additional mass of the dampers as a proportion of the native structure's mass.

A second comparison was made in which the thickness of the viscoelastic material in both dampers was varied and the modal loss factors calculated using both the Modal Strain Energy approach [23] and the Half-Power Bandwidth method [24]. The thickness of the viscoelastic layer was increased

from 0.2 to 2.7mm for the CLDs and from 0.25 to 2.33mm for the DSLJ inserts. The loss efficiency E_η was defined similarly as:

$$E_\eta = \frac{\eta_1}{m_a} \quad (2)$$

Where η_1 is the modal loss factor of the first mode and m_a is the additional mass of the dampers as a proportion of the native structure's mass.

3. Results

The present finite element model was benchmarked against the work by Chia *et al.* [16], in which they predicted a loss factor ratio per unit mass of 1.3477 (see Table 2 in [16]) for one CLD configuration (see Fig.7 in [16]). The same configuration modelled in this study predicted a loss factor ratio per unit mass of 1.3454. This close match demonstrated the present model's suitability for simulating the damping mechanism of the CLD and by extension the DSLJ.

3.1. Parametric optimisation of the DSLJ inserts

An initial static analysis showed that for the 270 mm long cantilevered beam model, the tip displacement required for the DSLJ insert to come into contact with the upper or lower skin was approximately 80 mm, and so such contact was not considered any further. Fig. 3 shows the loss efficiency E_η vs the added mass in percent as the honeycomb cells were filled rows by rows with DSLJ inserts for all structures. For all structures the peak loss efficiency was identified when only one row was filled with DSLJ inserts. It then decreased rapidly as more rows of cells were filled. A compromise solution was selected arbitrarily between maximal loss efficiency and maximal added mass, specifically was 5 rows filled with inserts (out of 17) for the beams and 6 rows filled (out of 19) for the plates. These configurations were used in further comparisons.

The effect of viscoelastic thickness on the loss efficiency E_η in the DSLJ is shown in Fig. 4. There is an inverse relationship between the thickness of the viscoelastic element and the loss efficiency in the DSLJ. The thickness of the DSLJ damper affects rapidly its performance, and whilst the optimal thickness within this study was 0.5 mm, it seems likely that even thinner solutions would have higher damping efficiencies. The configurations with the thinnest viscoelastic layer were selected for the later comparison. These selected configurations on cantilever beam, simply supported beam, cantilever plate and simply supported plate exhibited a peak modal loss factor of 1.52×10^{-3} , 1.34×10^{-3} , 1.66×10^{-3} and 1.50×10^{-3} respectively.

3.2. CLD and DSLJ dampers comparison

3.2.1. Amplitude and frequency comparison

The first mode amplitudes of the CLD and DSLJ configurations are shown in Figs. 5 to 8, with the undamped beam or plate for comparison. In the Figs. 5a to 8a the amplitude is shown vs frequency in absolute units, whereas in Figs. 5b to 8b it is shown vs frequency normalised to the natural frequency of each case (ω), in order to show more clearly the individual differences in amplitude response. In most cases the dampers reduced amplitude vs the undamped structures, as would be expected. The DSLJ was competitive in all case and even showed the largest amplitude reduction in the simply supported beam and cantilever plate configuration, see Fig. 6 and 7. It exhibits an amplitude reduction of 64% (cantilever beam), 53% (simply supported beam), 67% (cantilever plate) and 54% (simply supported plate) from the undamped configuration. The amplitude reduction efficiency E_a of DSLJ is 18, 24, 3 and 4 times higher than the best CLD configuration on the cantilever beam, simply supported beam, cantilever plate and simply supported plate respectively, see table 3. It can be seen that the high amplitude reduction efficiency noted for the DSLJ configuration correlates with a high strain energy density in the viscoelastic material.

In most cases the dampers also produced a decrease in natural frequency, with some cases showing large reductions, e.g. the CLD configuration by Ling [21] reduced frequency by almost 44%, see Fig. 7a. In almost all cases, the DSLJ damper produced the least change in natural frequency, except for the simply supported case where the natural frequency was reduced by 14%. In three cases the frequency was increased by the damper, and the ratio of modal stiffness to modal mass for these cases was larger vs the undamped versions; the DSLJ cantilevered beam (Fig. 4a), the Kim CLD [18] and DSLJ cantilevered plate (Fig. 6a).

3.2.2. Loss efficiency comparison

The loss efficiencies E_η for the CLD and DSLJ in all of the structures along with their added masses as a percentage of the total mass of the undamped structure are shown in Figs. 9 to 12. In all cases and for all types of dampers, the loss efficiency E_η decreased as the thickness of the viscoelastic layer was increased. DSLJ configurations were generally lighter and more efficient at low added mass than CLD configurations, except for the simply supported plate case where the CLD configuration proposed by Chen and Huang [15] achieved comparable loss efficiency at lower added mass. For example the DSLJ was more than 5 times more efficient than the best CLD damper for the cantilevered beam, see Fig. 9. The stars on Figs. 9 to 12 indicate the added mass of the CLD configuration as proposed in the original study where those authors considered the thickness of the viscoelastic layer as an optimisation parameter. In these cases there are CLD configurations identified here which were more efficient than those originally identified by the authors, for example the CLD configuration as proposed by Hou [20] was more efficient with a thinner viscoelastic layer, see Fig. 12. Table 4 gives the values for peak modal loss factor, relative added mass and loss efficiency at peak amplitude for all configurations. The two techniques used to calculate the modal loss factor, i.e. the Modal Strain Energy and the Half-Power Bandwidth methods, demonstrated very similar results.

4. Discussion

The parametric optimisation of the DSLJ revealed that a single row of inserts is the most efficient for both cantilevered and simply supported structures, and a small number of inserts (5 or 6 rows in these cases) is a good compromise between peak loss efficiency E_η , large modal loss factor and added mass, see Fig. 3. The DSLJ was most effective when the viscoelastic layer was thin, see Fig. 4. For a given global deformation the strain energy density in the viscoelastic layer was higher when the layer was thinner. There will likely be some practical manufacturing limits on the thickness of the viscoelastic layer, as well as other possible limits arising from the ultimate shear strain and adhesive strength of the viscoelastic material.

The DSLJ were best for amplitude reduction for most configurations though not all, and were competitive with all the CLD configurations, in both absolute and mass efficient reduction. This is due to the fact that the strain energy in the viscoelastic material was usually higher in the DSLJ than in a CLD for a given global strain (see table 3). The DSLJ therefore appeared to be a more effective way of packing in viscoelastic material in order to reach a higher loss factor. The exceptions were Hajela and Lin [11] and Zheng [22] in the cantilevered beam and simply supported plate cases, both of which showed the highest amplitude reduction. However this was at the cost of high added mass and coverage of most the surface. Indeed, the amplitude reduction efficiency E_a was always the highest for all configurations. The hybrid CLD proposed by Hau [29], which was never designed to operate purely passively, did not perform well in comparison to other configurations.

In most cases the dampers reduced the natural frequency as might be expected. In some notable cases however the dampers raised the ratio of modal stiffness to modal mass and therefore the resonance frequency (see Figs. 5a and 7a). With weight efficient dampers it should be possible in many cases to conserve initial modal frequencies when adding dampers.

There was an inverse relationship between the loss efficiencies E_η for both the CLD and DSLJ and the viscoelastic layer thickness, see Figs. 9 to 12. The thickness of the viscoelastic layer was the primary determinant of the strain and strain energy density in the viscoelastic layer, and thus efficiency of the dampers in this study using both the Modal Strain Energy and Half-Power Bandwidth methods. The loss efficiency is very sensitive to the DSLJ thickness.

As with amplitude reduction the data for loss efficiency indicate that DSLJ tend to be more efficient because the viscoelastic layer sees higher strains for given global deformations. For example, the DSLJ had a loss factor of almost twice of that of the Hou CLD configurations (1.14×10^{-3} and 5.62×10^{-4} for the DSLJ and CLD configurations respectively), see Fig. 10. The exception was in the simply supported plate with the configuration of Chen [15], i.e. a small patch in the centre of the plate, which was more mass efficient than the DSLJ, see Fig. 12 and table 4.

In the DSLJ arrangement the viscoelastic is located in two layers, both of which are under strain. In contrast in the CLD arrangement the viscoelastic is placed in one layer. Thus for a similar mass, the viscoelastic in the DSLJ arrangement experiences a higher strain because it is arranged in thinner layers than in a CLD. Clearly by placing thinner CLD patches on upper and lower surfaces this advantage can be overcome, though for many practical reasons this may not always be possible.

Moreover, the DSLJ is sensitive to both internal shear and flexure of the base structure whereas the CLD's shearing mechanism is only due to flexure. Hence for applications where the lightweight properties are critical, the DSLJ damper can be an efficient alternative to the CLD.

5. Conclusion

This paper presents the performance of a new kind of viscoelastic damper for honeycomb sandwich structures and compares its efficiency to benchmarked optimal configurations of CLDs on beam and plate structures. It provides the reader with a parametrically optimised configuration for DSLJ dampers for beams and plates structures under both cantilever and simply supported boundary condition.

The new DSLJ inserts exhibit an excellent ability to damp vibrations for small increases in mass, in terms of both amplitude reduction and modal loss factor. They also generally produce a smaller shift in natural frequency from the undamped structure which may be an important asset for many transport applications. Therefore, DSLJ inserts represent a competitive alternative to CLDs. Since they are internal to the honeycomb cell, they can be implemented in applications where adding dampers externally is difficult. This may be the case for gas turbine blades with large internal void spaces convenient for DSLJ deployment, but which cannot have external dampers interfering with air flow. If deployed in honeycombs, the orientation of the DSLJ damper can be altered, raising the possibility for tuning of orientation according to global vibration modes.

6. Acknowledgements

This work was supported by the MEET project (Material for Energy Efficiency in Transport) in the context of the INTERREG IV A France (Channel) – England European cross-border co-operation programme, which is co-financed by the ERDF.

7. References

- [1] L. J. Gibson and M. F. Ashby, *Cellular Solids: Structure and Properties*. Cambridge University Press, 1999.
- [2] D. I. G. Jones, *Handbook of viscoelastic vibration damping*. Chichester; New York: J. Wiley, 2001.
- [3] F. Agnese and F. Scarpa, 'Macro-composites with star-shaped inclusions for vibration damping in wind turbine blades', *Compos. Struct.*, vol. 108, pp. 978–986, Feb. 2014.
- [4] R. Rajasekaran, F. Scarpa, C. Smith, W. Miller, and K. Evans, 'Vibration Damping Structures', WO/2011/104112, 02-Sep-2011.
- [5] M.-A. Boucher, C. W. Smith, F. Scarpa, R. Rajasekaran, and K. E. Evans, 'Effective topologies for vibration damping inserts in honeycomb structures', 2012.
- [6] G. J. Murray and F. Gandhi, 'Auxetic honeycombs with lossy polymeric infills for high damping structural materials', *J. Intell. Mater. Syst. Struct.*, vol. 24, no. 9, pp. 1090–1104, Jun. 2013.
- [7] R. Rajasekaran, M.-A. Boucher, F. Scarpa, and K. Evans, 'Vibration damping', US 2013/0264757 A1, 10-Oct-2013.
- [8] J. Edward M. Kerwin, 'Damping of Flexural Waves by a Constrained Viscoelastic Layer', *J. Acoust. Soc. Am.*, vol. 31, no. 7, pp. 952–962, 1959.
- [9] N., F. C. Nokes, D.S., 'Constrained layer damping with partial coverage', *Shock Vib. Bull.*, vol. 68, no. part 3.
- [10] J. M. Lifshitz and M. Leibowitz, 'Optimal sandwich beam design for maximum viscoelastic damping', *Int. J. Solids Struct.*, vol. 23, no. 7, pp. 1027–1034, 1987.
- [11] P. Hajela and C.-Y. Lin, 'Optimal Design of Viscoelastically Damped Beam Structures', *Appl. Mech. Rev.*, vol. 44, no. 11S, p. S96, 1991.
- [12] J.-L. Marcelin, P. Trompette, and A. Smati, 'Optimal constrained layer damping with partial coverage', *Finite Elem Anal Des*, vol. 12, no. 3–4, pp. 273–280, Dec. 1992.
- [13] H. Zheng, G. S. H. Pau, and Y. Y. Wang, 'A comparative study on optimization of constrained layer damping treatment for structural vibration control', *Thin-Walled Struct.*, vol. 44, no. 8, pp. 886–896, Aug. 2006.
- [14] H. Zheng, C. Cai, and X. M. Tan, 'Optimization of partial constrained layer damping treatment for vibrational energy minimization of vibrating beams', *Comput. Struct.*, vol. 82, no. 29–30, pp. 2493–2507, Nov. 2004.
- [15] Y.-C. Chen and S.-C. Huang, 'An optimal placement of CLD treatment for vibration suppression of plates', *Int. J. Mech. Sci.*, vol. 44, no. 8, pp. 1801–1821, Aug. 2002.
- [16] C. M. Chia, J. A. Rongong, and K. Worden, 'Strategies for using cellular automata to locate constrained layer damping on vibrating structures', *J. Sound Vib.*, vol. 319, no. 1–2, pp. 119–139, Jan. 2009.
- [17] C. M. Chia, J. A. Rongong, and K. Worden, 'Evolution of constrained layer damping using a cellular automaton algorithm', *Proc. Inst. Mech. Eng. Part C J. Mech. Eng. Sci.*, vol. 222, no. 4, pp. 585–597, Apr. 2008.
- [18] S. Y. Kim, 'Topology design optimization for vibration reduction: reducible design variable method.', Queen's University, Kingston, Ontario, Canada, 2011.
- [19] S. W. Hou, Y. H. Jiao, and Z. B. Chen, 'Optimum Layout of Partially Covered Sandwich Beam with Constrained Layer Damping', *Appl. Mech. Mater.*, vol. 66–68, pp. 588–593, Jul. 2011.
- [20] S. W. Hou, Y. H. Jiao, X. Wang, Z. B. Chen, and Y. B. Fan, 'Optimization of Plate with Partial Constrained Layer Damping Treatment for Vibration and Noise Reduction', *Appl. Mech. Mater.*, vol. 138–139, pp. 20–26, Nov. 2011.
- [21] Z. Ling, X. Ronglu, W. Yi, and A. El-Sabbagh, 'Topology optimization of constrained layer damping on plates using Method of Moving Asymptote (MMA) approach', *Shock Vib.*, vol. 18, no. 1, pp. 221–244, Jan. 2011.

- [22] W. Zheng, Y. Lei, S. Li, and Q. Huang, 'Topology optimization of passive constrained layer damping with partial coverage on plate', *Shock Vib.*, vol. 20, no. 2, pp. 199–211, 2013.
- [23] C. D. Johnson and D. A. Kienholz, 'Finite Element Prediction of Damping in Structures with Constrained Viscoelastic Layers', *AIAA J.*, vol. 20, no. 9, pp. 1284–1290, 1982.
- [24] S. S. Rao, *Mechanical vibrations*. Upper Saddle River, N.J.: Prentice Hall, 2011.
- [25] S. Srinivas, C. V. Joga Rao, and A. K. Rao, 'An exact analysis for vibration of simply-supported homogeneous and laminated thick rectangular plates', *J. Sound Vib.*, vol. 12, no. 2, pp. 187–199, Jun. 1970.
- [26] F. P. Landi, F. Scarpa, J. A. Rongong, and G. R. Tomlinson, *Improving the MSE method for damped structures*. Heverlee: Katholieke Univ Leuven, Dept Werktuigkunde, 2001.
- [27] B. E. Douglas and J. C. S. Yang, 'Transverse compressional damping in the vibratory response of elastic-viscoelastic-elastic beams', *AIAA J.*, vol. 16, no. 9, pp. 925–930, 1978.
- [28] ANSYS® Academic Research, Release 14.0, 'Ansys Help System, Mechanical APDL, Theory Reference'.
- [29] L. C. Hau and E. H. K. Fung, 'Multi-objective optimization of an active constrained layer damping treatment for shape control of flexible beams', *Smart Mater. Struct.*, vol. 13, no. 4, p. 896, Aug. 2004.

8. Figure captions

Fig. 1: A typical constrained layer damper, Figs. 1a and 1b, and a double shear lap-joint damper inserted in a hexagonal honeycomb cell, Figs. 1c and 1d. The structures shown in 1b and 1d are deformed under load.

Fig. 2: Honeycomb-cored sandwich beam, with upper skin removed for clarity.

Fig. 3: Loss efficiency E_η vs the additional mass as a percentage of the total mass of the undamped structure, as rows of cells are filled sequentially with DSLJ inserts on all structures.

Fig. 4: Loss efficiency E_η vs the additional mass as a percentage of the total mass of the undamped structure, as thickness of the viscoelastic element is increased from 0.25 to 2.33mm.

Fig. 5a: The amplitude of the cantilever beams excited at their first modes. The vibration amplitude (X) of each structure is normalised to that of the undamped structure (X_0). Fig. 5b: Detail of the distribution of the vibration amplitude about each resonant frequency.

Figs. 6a and 6b: As per Figs. 5a and 5b but for the simply supported beam.

Figs. 7a and 7b: As per Figs. 5a and 5b but for the cantilever plate.

Figs. 8a and 8b: As per Figs. 5a and 5b but for the simply supported plate.

Fig. 9: Comparison of the loss efficiency E_η vs added mass for the cantilever beam solutions.

Fig. 10: Comparison of the loss efficiency E_η vs added mass for the simply supported beam solutions.

Fig. 11: Comparison of the loss efficiency E_η vs added mass for the cantilever plate solutions.

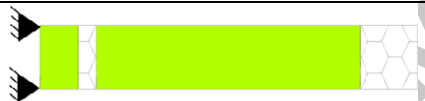

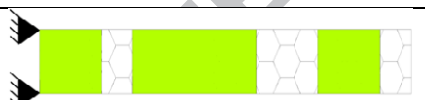



Fig. 12: Comparison of the loss efficiency E_η vs the proportional added mass for the simply supported plate solutions.


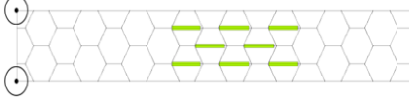
9. Table captions

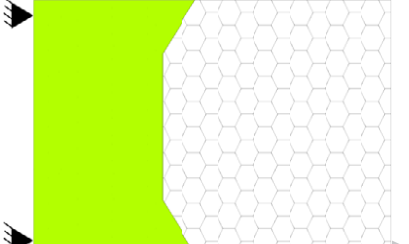
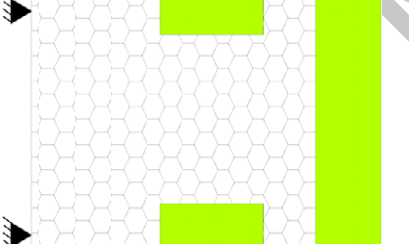
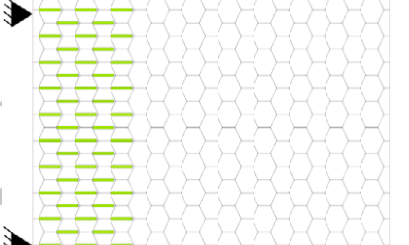
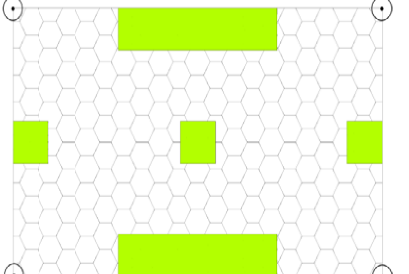
Table 1: Material parameters. The viscoelastic material properties are.

	Base structure	Viscoelastic layer	Constraining layer
Density (kg/m^3)	2700	1000	2700
Material loss factor	0.0005	0.1	0.0005
Young's modulus (MPa)	70 000	1	70 000
Poisson's ratio	0.33	0.45	0.33

Table 2: Benchmarked optimised damper configurations for beam (a) and plate (b) structures. The sandwich skins are shown removed for clarity. The presence of a damper is given by solid colouring (CLD) or inserts in cells (DSLJ). Boundary conditions are indicated by solid triangles (encastred) and open circles (pinned) for the cantilever and simply supported cases respectively. *These solutions are for hybrid dampers.

Adapted from	Damper location and geometry	Optimisation technique	Objective function	Penalty function	Design Variables
Hajela and Lin [11]		Genetic algorithm	Modal loss factor	Added mass	CLD location
Marcelin <i>et al.</i> [12]		Method of the Moving Asymptotes	Modal loss factor	No penalty function	CLD location
Hau [29]*		Multi-objective genetic algorithm	Total weight, control voltages	Damping ratio of the first three modes	CLD location and length
Double shear lap-joint (cantilever beam) [5]			Modal loss factor	Added mass	DSLJ location
Pau, Zheng, Wang [13]		Sequential Quadratic Programming	Amplitude reduction	Added mass	CLD location and length
Zheng, Cai, Tan [14]		Genetic algorithm	Vibrational energy	Added mass	CLD location and length

Hou, Jiao, Chen [19]		Genetic algorithm	Modal loss factor	Added volume	CLD location, layer thicknesses, shear modulus
Double shear lap-joint (simply supported beam) [5]			Modal loss factor	Added mass	DSLJ location

Adapted from	Damper location and geometry	Optimisation technique	Objective function	Penalty function	Design Variables
Kim [18]		Evolutionary Structural Optimisation	Modal loss factor	Added volume	CLD location
Ling <i>et al.</i> [21]		Method of the Moving Asymptotes	Modal damping ratio	Added mass	CLD location
Double shear lap-joint (cantilever plate) [5]			Modal loss factor	Added mass	DSLJ location
Ling <i>et al.</i> [21]		Method of the Moving Asymptotes	Modal damping ratio	Added mass	CLD location

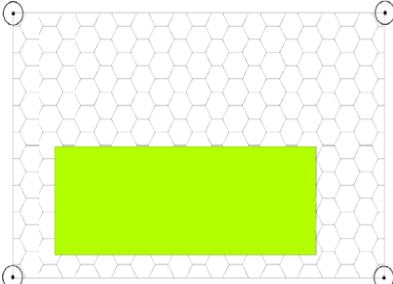
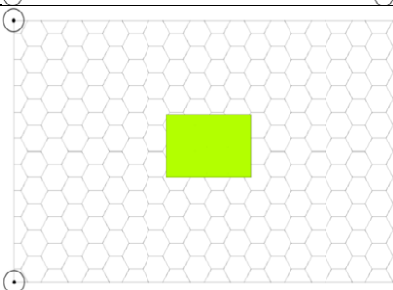
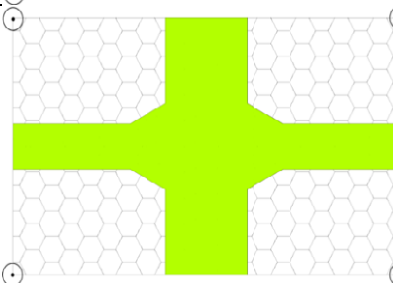
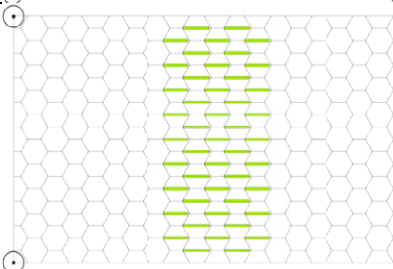
Hou, Jiao, Wang [20]		Genetic algorithm	Vibrational energy	Added mass	CLD location, layer thicknesses, shear modulus
Chen and Huang [15]		Topographic method	Structural damping ratio	Resonant frequency shift	CLD location, layer thicknesses
Zheng et al. [22]		Method of Moving Asymptote	Modal loss factor	Added mass	CLD location
Double shear lap-joint (simply supported plate) [5]			Modal loss factor	Added mass	DSLJ location

Table 3: Relative amplitude reduction, additional mass, amplitude reduction efficiency and strain energy density in the viscoelastic material at peak amplitude for all configurations. The amplitude reduction and amplitude reduction efficiency are relative to the undamped structure. The strain energy density in the viscoelastic material is relative to that of the DSLJ structure. * Indicates hybrid solutions.

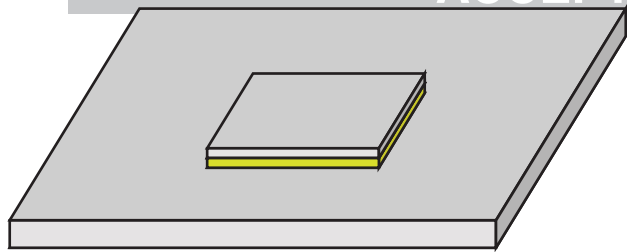
Cantilever beam	Relative amplitude reduction to the undamped structure (%)	Additional mass relative to the undamped structure (%)	Amplitude reduction efficiency E_a	Strain energy density in the viscoelastic material normalised to the DSLJ (%)
Hajela and Lin [11]	73	287	0.25	1.61
Marcelin <i>et al.</i> [12]	31	151	0.21	9.68
Hau [28]*	31	128	0.24	13.09
Double shear lap-joint [5]	64	14	4.57	100
Simply supported beam	Relative amplitude reduction to the undamped structure (%)	Additional mass relative to the undamped structure (%)	Amplitude reduction efficiency E_a	Strain energy density in the viscoelastic material normalised to the DSLJ (%)
Pau, Zheng, Wang [13]	9	117	0.08	19.17
Zheng, Cai, Tan [14]	21	179	0.12	46.99
Hou, Jiao, Chen [19]	11	70	0.16	207.21
Double shear lap-joint [5]	53	14	3.79	100
Cantilever plate	Relative amplitude reduction to the undamped structure (%)	Additional mass relative to the undamped structure (%)	Amplitude reduction efficiency E_a	Strain energy density in the viscoelastic material normalised to the DSLJ (%)
Kim [18]	56	67	0.84	31.05
Ling <i>et al.</i> [21]	52	196	0.26	6.65
Double shear lap-joint [5]	67	19	3.53	100
Simply supported plate	Relative amplitude reduction to the undamped structure (%)	Additional mass relative to the undamped structure (%)	Amplitude reduction efficiency E_a	Strain energy density in the viscoelastic material normalised to the DSLJ (%)
Ling <i>et al.</i> [21]	23	27	0.85	45.11
Hou, Jiao, Wang [20]	64	123	0.52	7.57
Chen and Huang [15]	12	19	0.63	63.11
Zheng <i>et al.</i> [22]	69	652	0.11	18.24
Double shear lap-joint [5]	54	19	2.84	100

Table 4: Modal loss factor and additional mass relative to the undamped structure at peak loss efficiency E_η for all configurations. The modal loss factor was estimated by means of both the Modal Strain Energy (MSE) and the Half-Power Bandwidth (HPB) methods. * Indicates a hybrid solution.

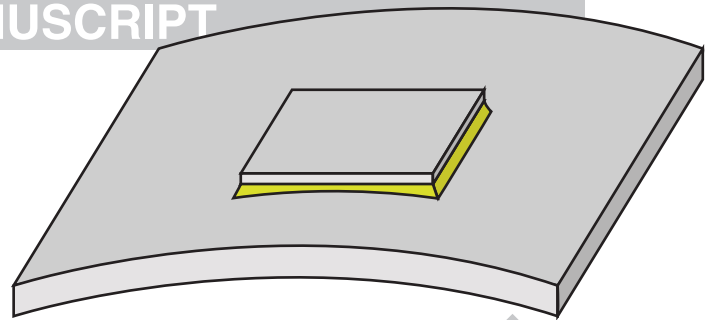
Cantilever beam	Modal loss factor at peak loss efficiency MSE ($\times 10^{-4}$)	Modal loss factor at peak loss efficiency HPB ($\times 10^{-4}$)	Added mass at peak loss efficiency (%)	Peak loss efficiency E_η ($\times 10^{-6}$)
Hajela and Lin [11]	5.19	5.65	71	7.31
Marcelin <i>et al.</i> [12]	5.25	5.62	33	15.8
Hau [28]*	6.10	7.33	11	47.1
Double shear lap-joint [5]	15.2	13.33	18	85.0
Simply supported beam	Modal loss factor at peak loss efficiency MSE ($\times 10^{-4}$)	Modal loss factor at peak loss efficiency HPB ($\times 10^{-4}$)	Added mass at peak loss efficiency (%)	Peak loss efficiency E_η ($\times 10^{-6}$)
Pau, Zheng, Wang [13]	5.29	5.45	11	47.1
Zheng, Cai, Tan [14]	5.00	5.08	18	27.1
Hou, Jiao, Chen [19]	5.03	5.11	10	48.7
Double shear lap-joint [5]	13.4	9.98	18	75.3
Cantilever plate	Modal loss factor at peak loss efficiency MSE ($\times 10^{-4}$)	Modal loss factor at peak loss efficiency HPB ($\times 10^{-4}$)	Added mass at peak loss efficiency (%)	Peak loss efficiency E_η ($\times 10^{-6}$)
Kim [18]	17.1	23.78	65	26.4
Ling <i>et al.</i> [21]	5.02	7.10	52	9.73
Double shear lap-joint [5]	16.6	14.33	23	70.8
Simply supported plate	Modal loss factor at peak loss efficiency MSE ($\times 10^{-4}$)	Modal loss factor at peak loss efficiency HPB ($\times 10^{-4}$)	Added mass at peak loss efficiency (%)	Peak loss efficiency E_η ($\times 10^{-6}$)
Ling <i>et al.</i> [21]	5.01	5.17	32	15.8
Hou, Jiao, Wang [20]	30.0	27.59	49	61.8
Chen and Huang [15]	5.00	5.15	8	59.2
Zheng <i>et al.</i> [22]	21.8	19.52	64	33.7
Double shear lap-joint [5]	15.0	10.63	23	64.0

Figure 1

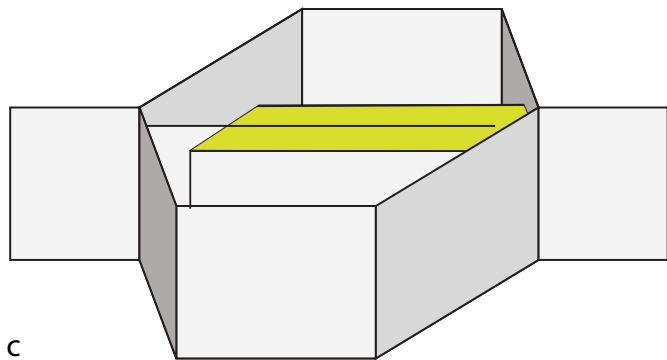
ACCEPTED MANUSCRIPT



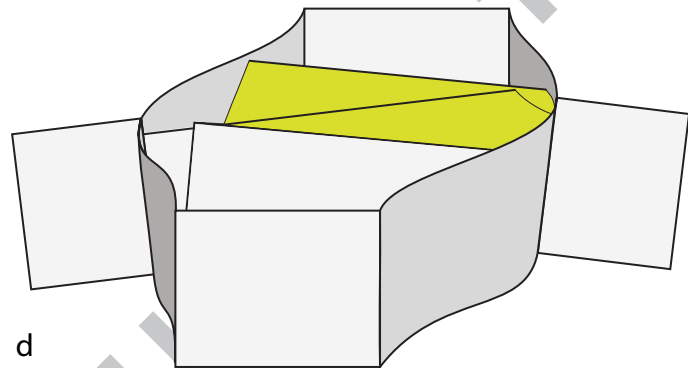
a



b



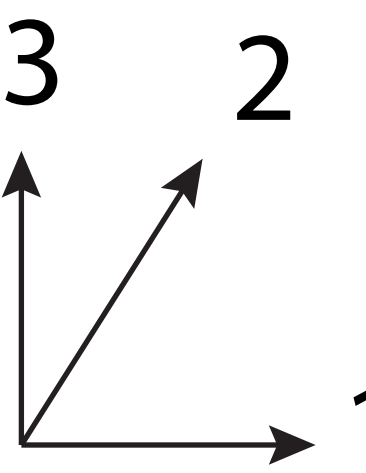
c



d

270 mm

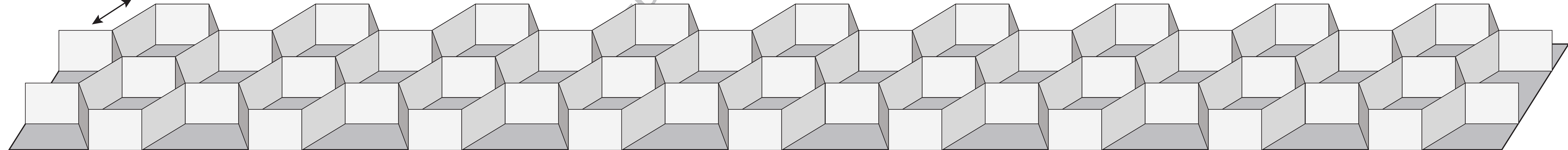
34.6 mm

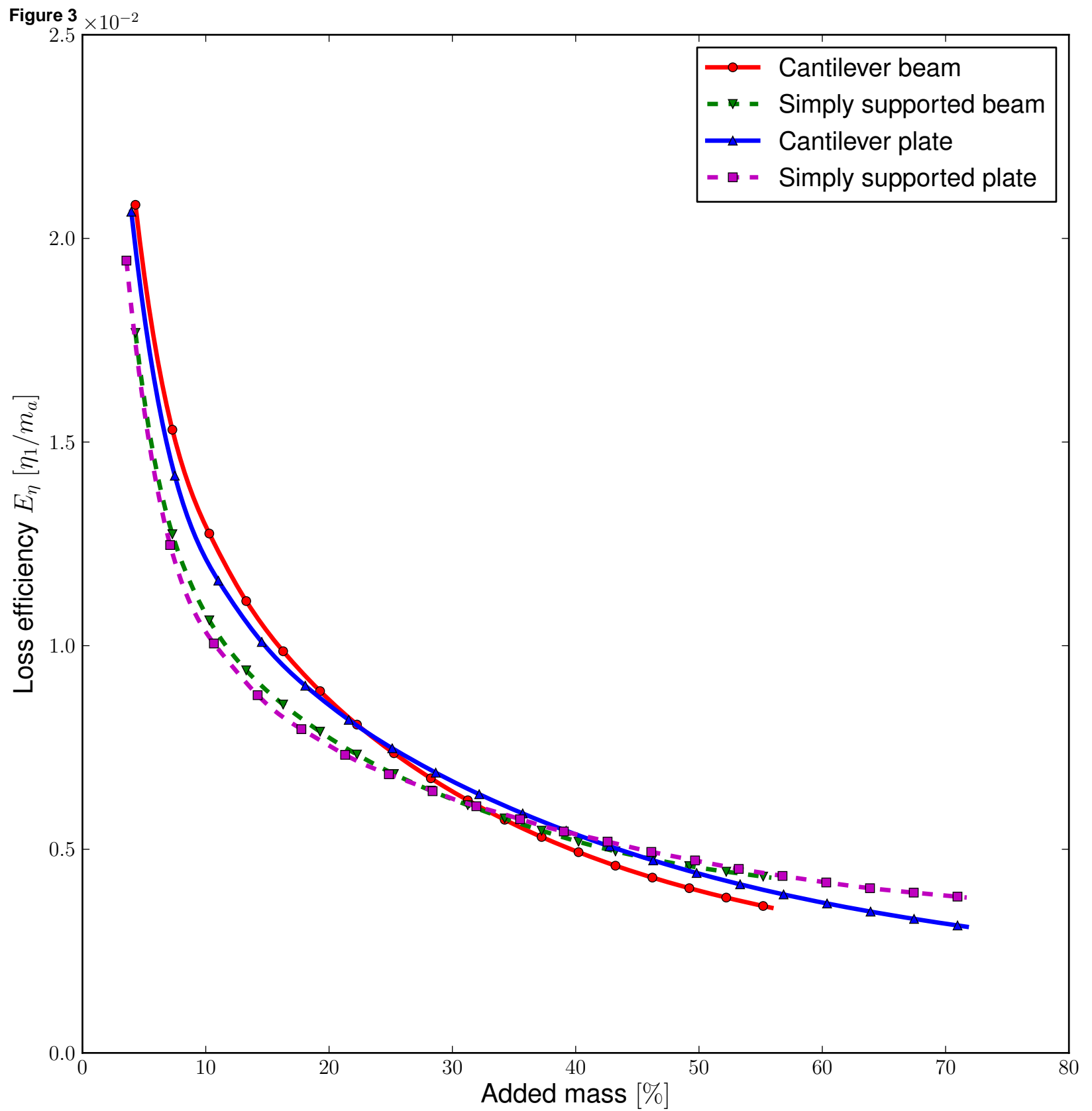


10 mm

10 mm

10 mm





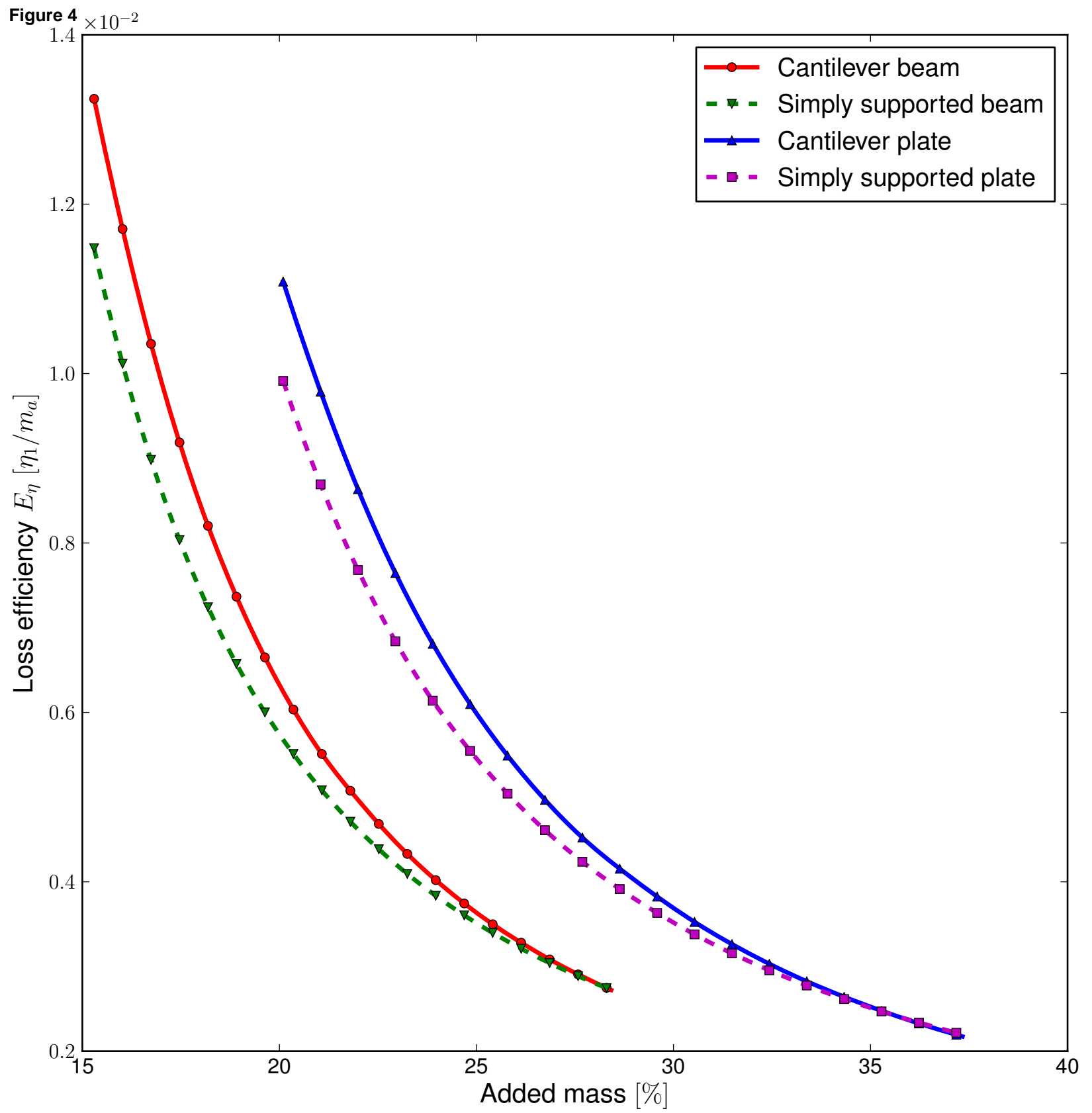


Figure 5a

Cantilever beam

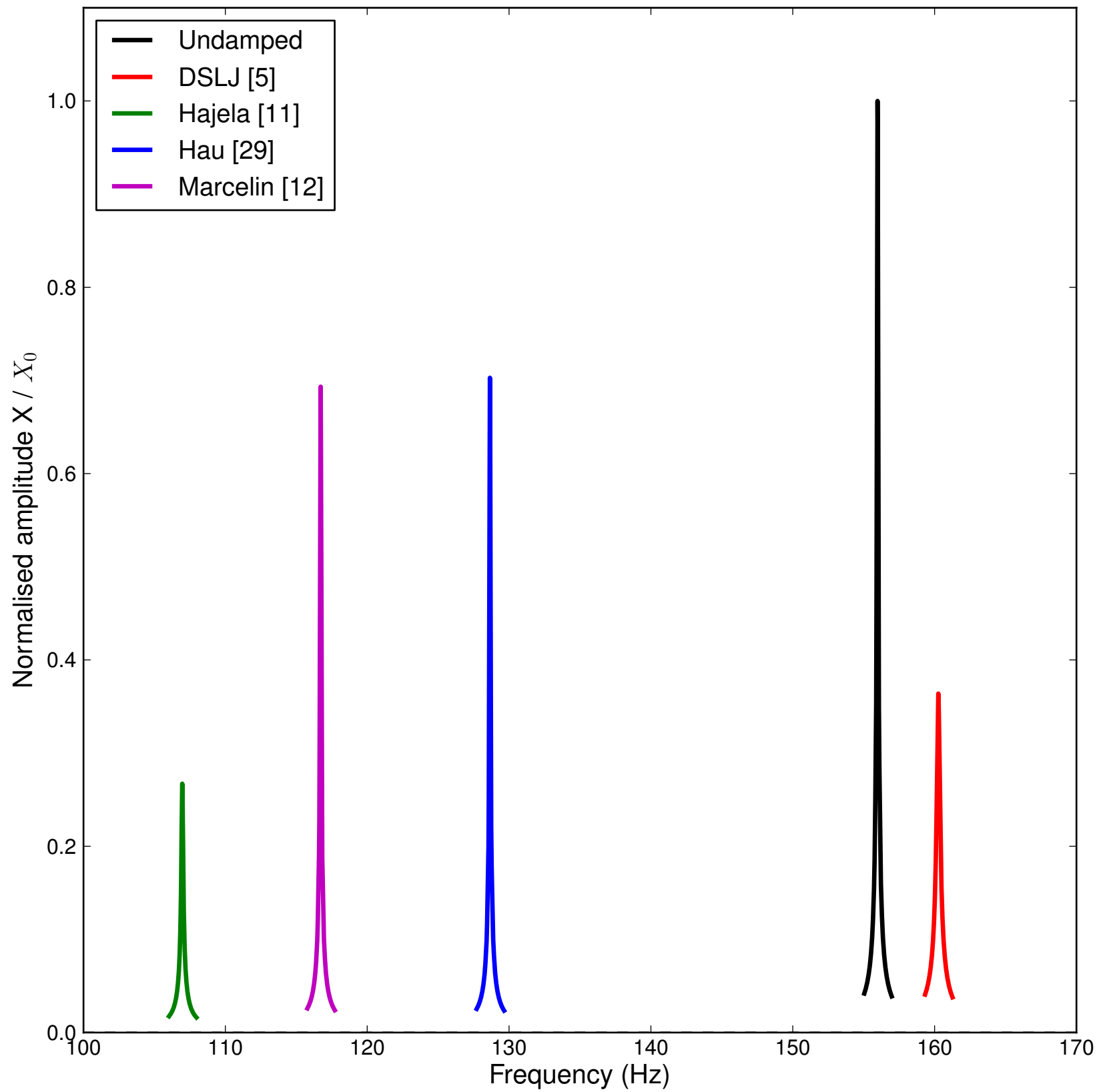


Figure 5b

Cantilever beam

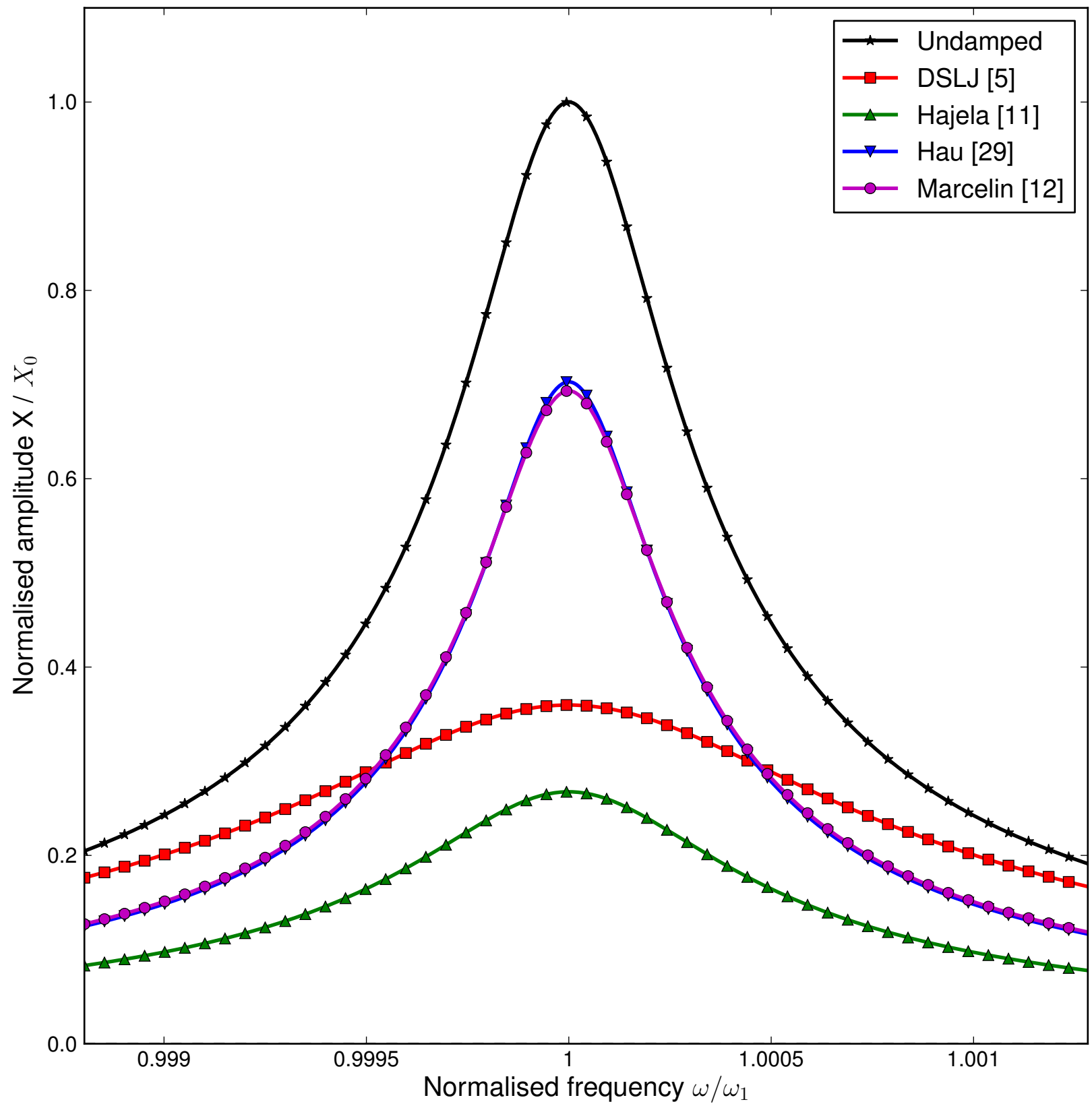


Figure 6a

Simply supported beam

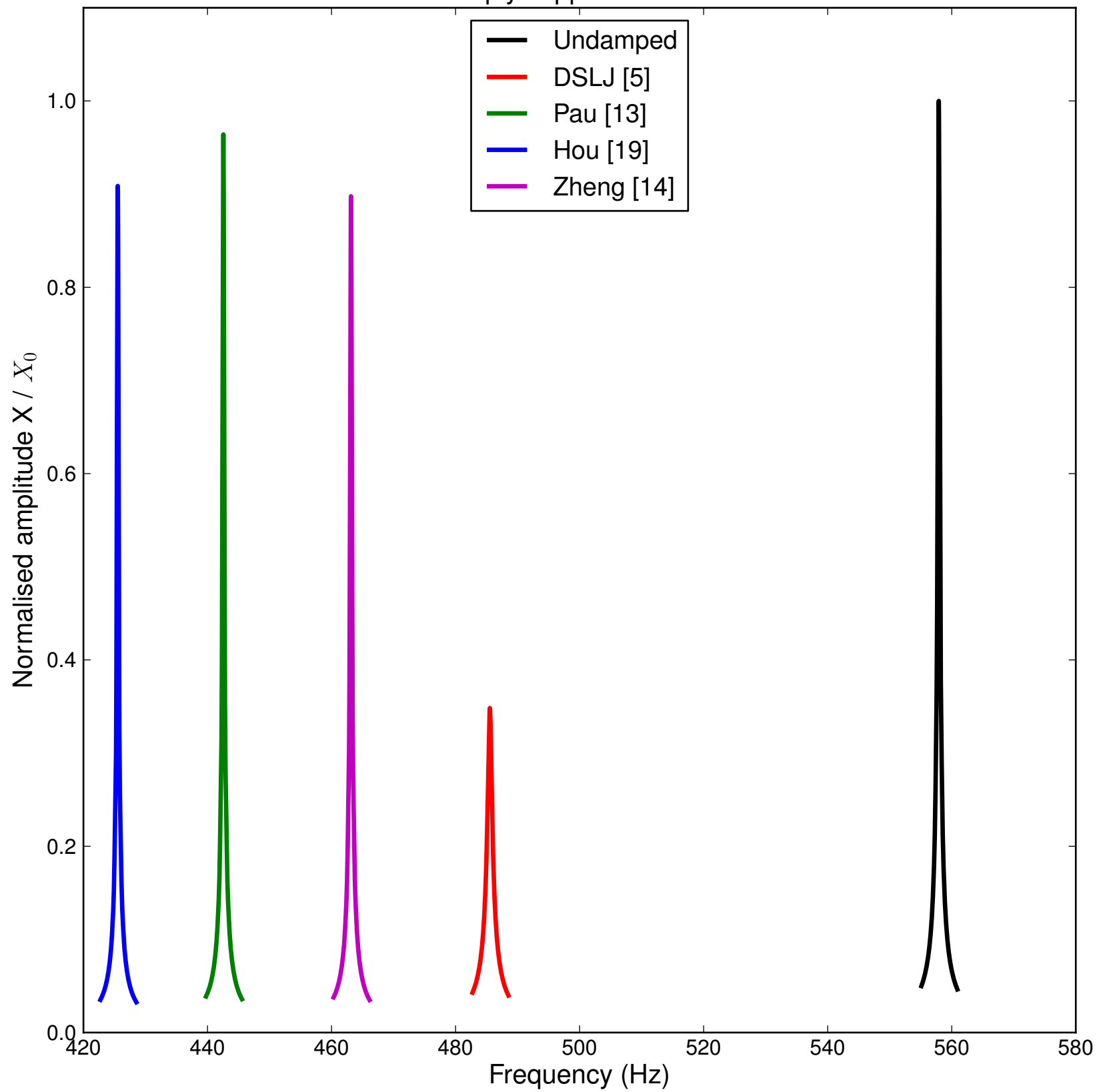


Figure 6b

Simply supported beam

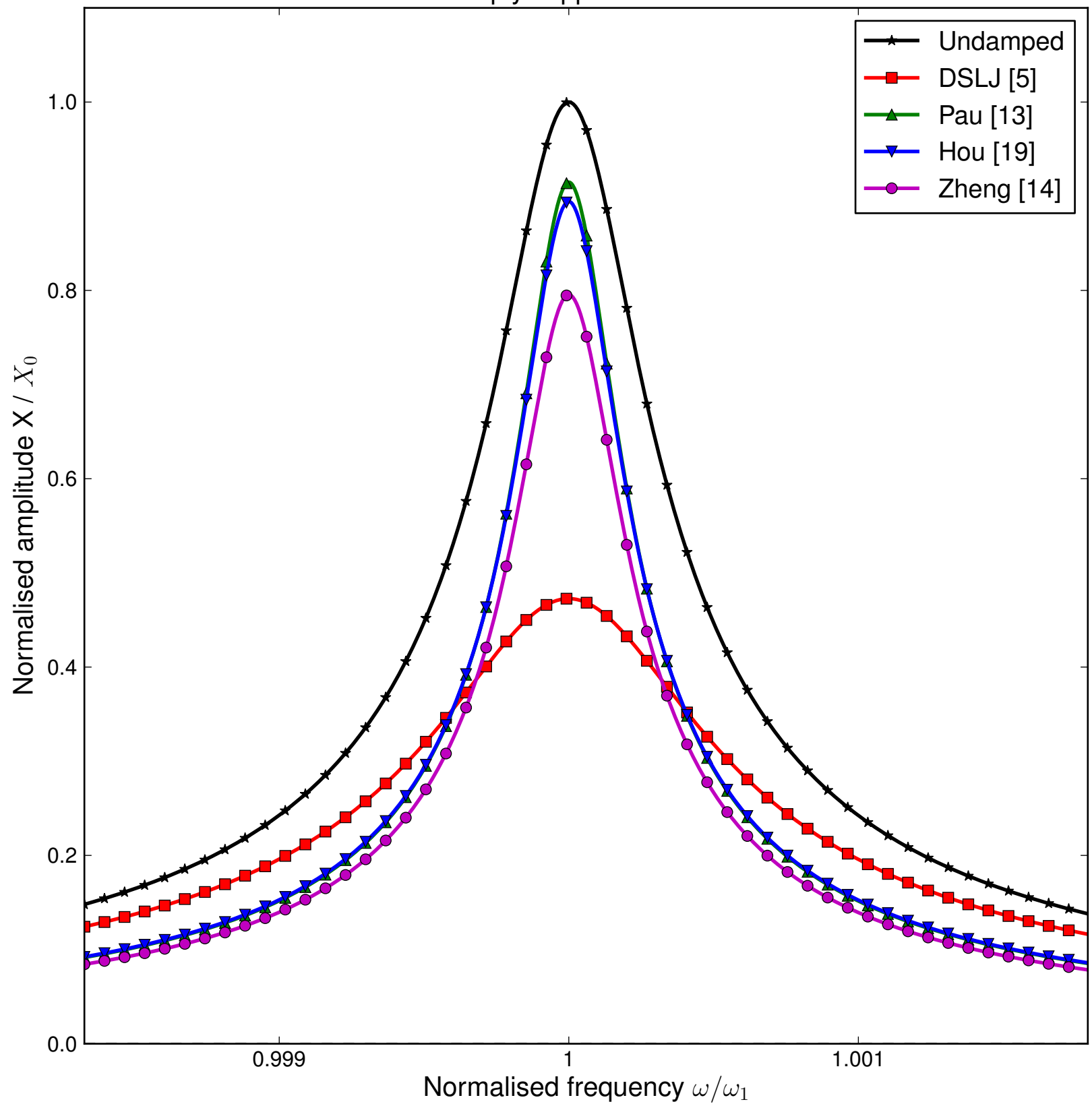


Figure 7a

Cantilever plate

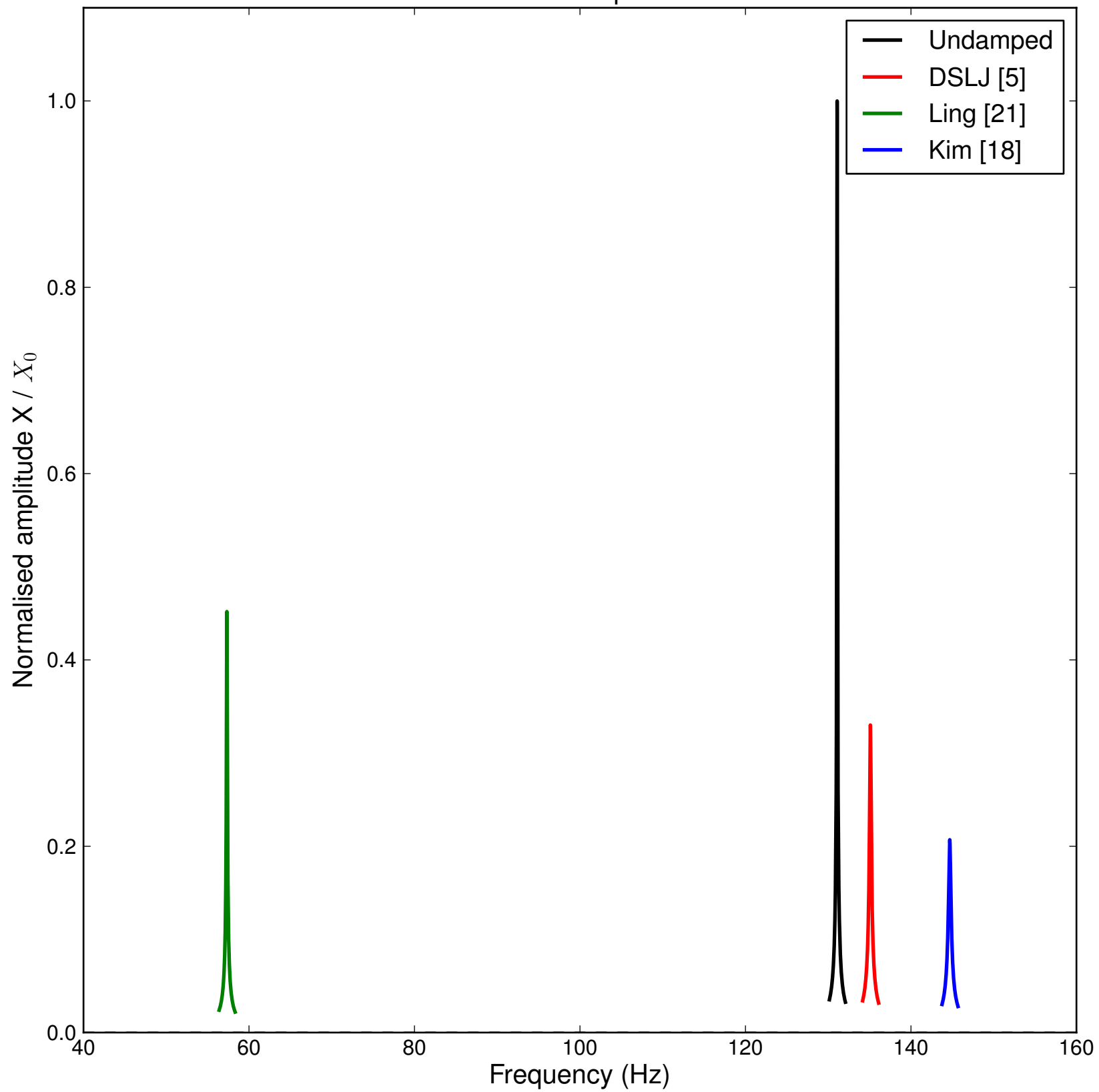


Figure 7b

Cantilever plate

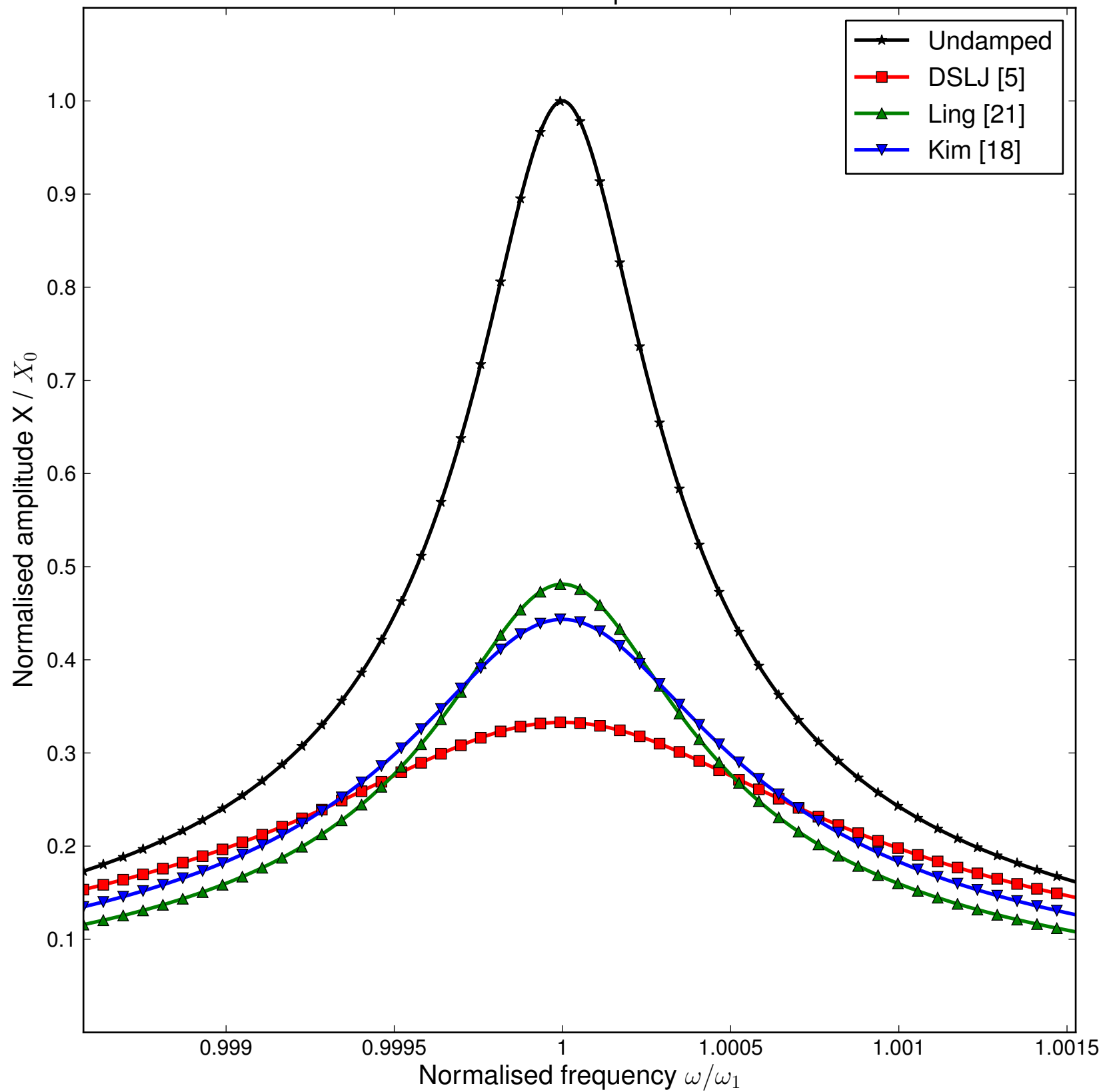


Figure 8a

Simply supported plate

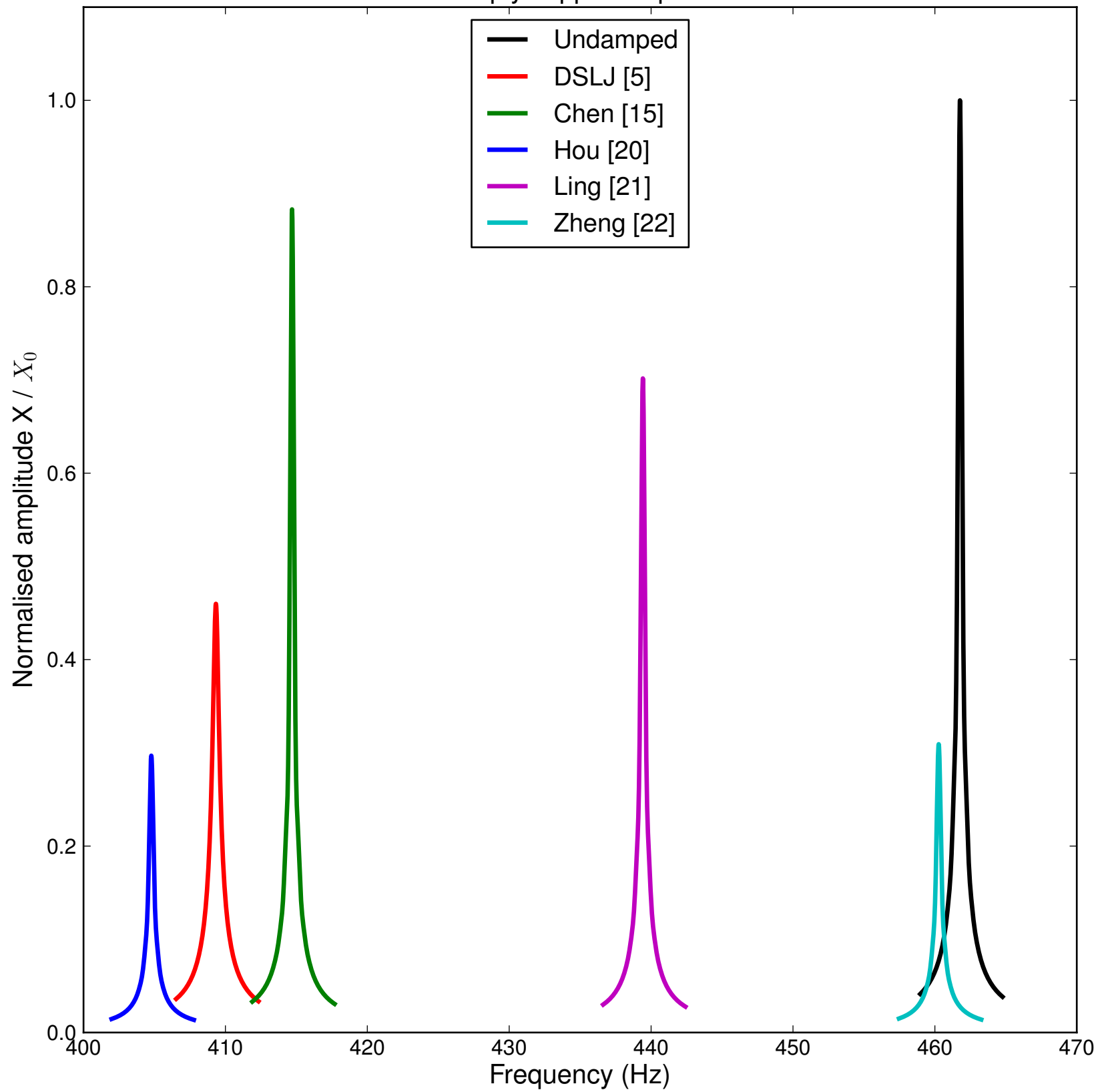


Figure 8b

Simply supported plate

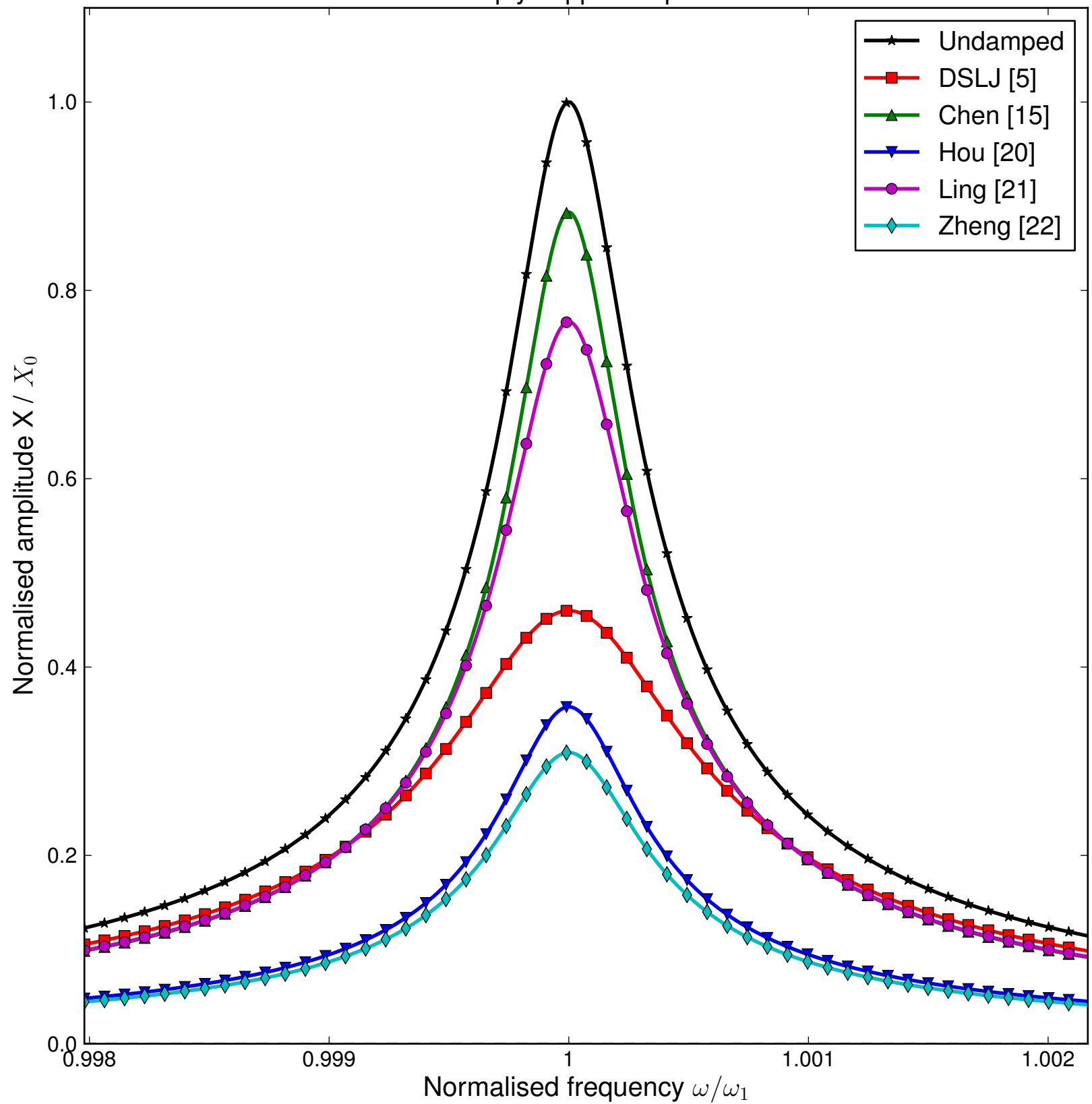


Figure 9

Cantilever beam

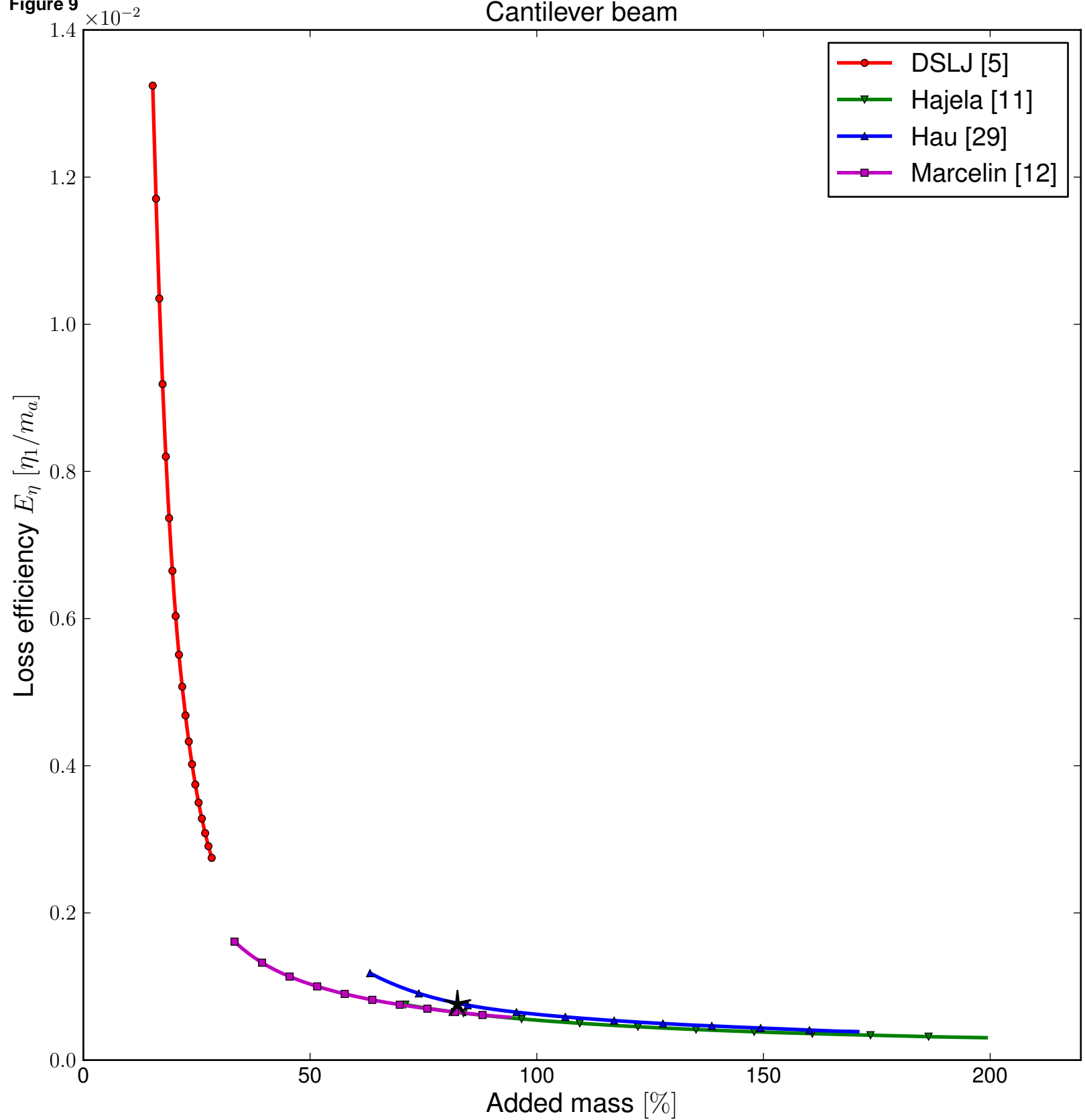
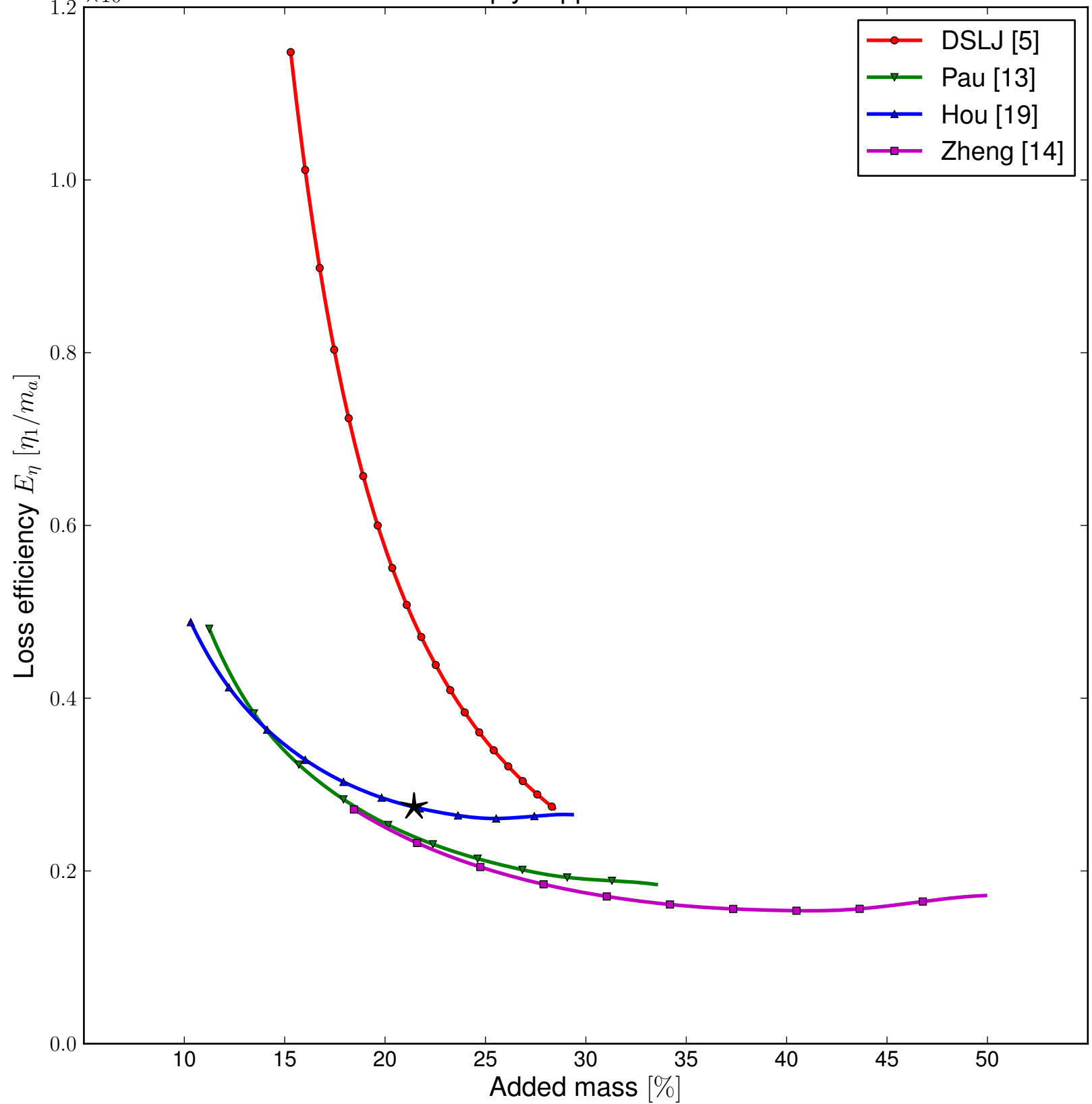


Figure 10 Simply supported beam



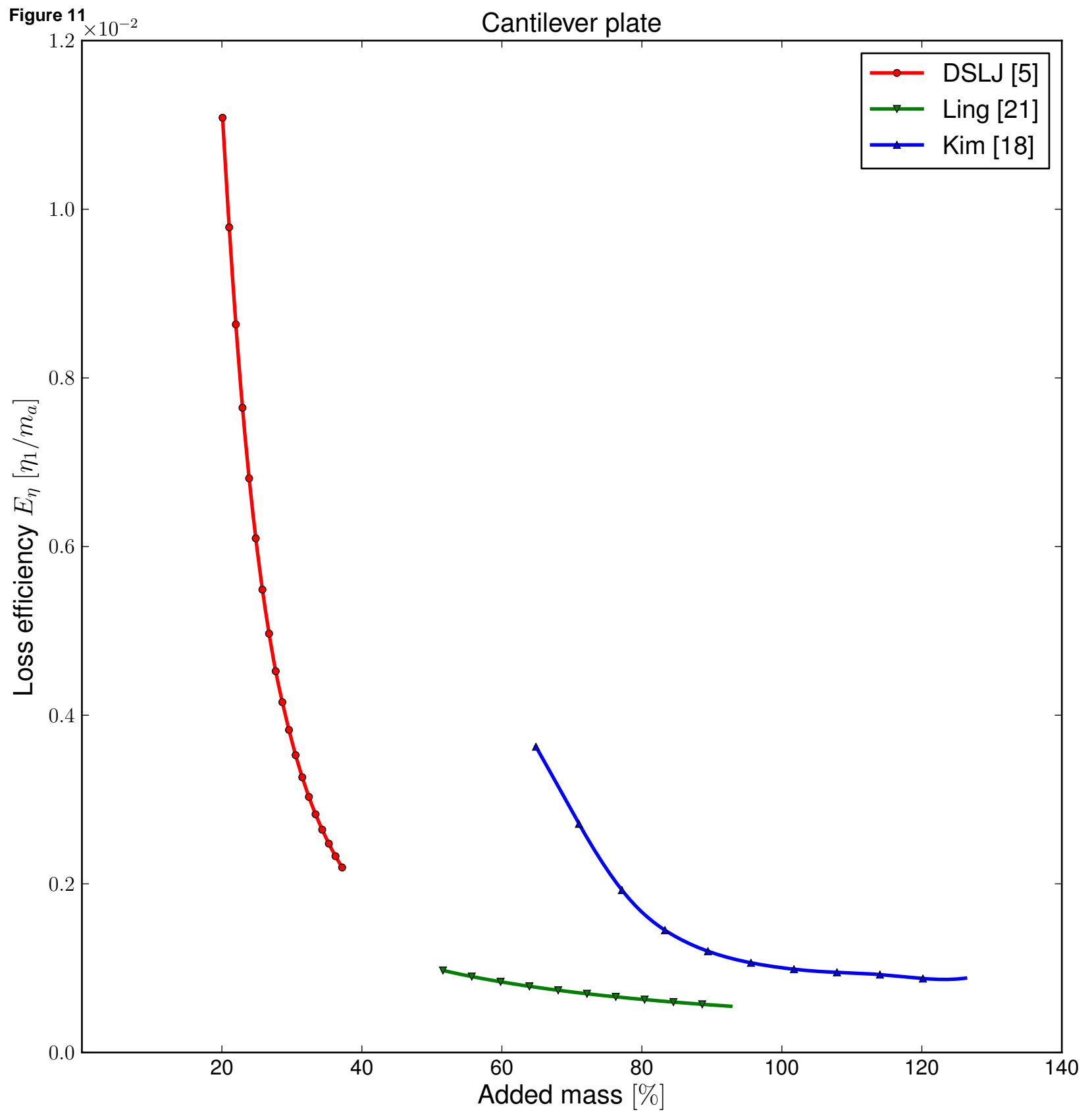


Figure 12 $\times 10^{-2}$ Simply supported plate

